

Effect of unequal load of carbon xerogel in electrodes on the electrochemical performance of asymmetric supercapacitors

E. G. Calvo · F. Lufrano · A. Arenillas ·
A. Brigandì · J. A. Menéndez · P. Staiti

Received: 5 August 2013 / Accepted: 13 December 2013 / Published online: 19 December 2013
© Springer Science+Business Media Dordrecht 2013

Abstract This paper investigates the electrochemical performance of asymmetric supercapacitors in an environmentally friendly aqueous electrolyte (1.0 mol L⁻¹ sodium sulfate solution). The asymmetric configuration is based on the use of a highly porous carbon xerogel as active material in both the positive and negative electrodes, but the carbon xerogel loading in each electrode has been substantially modified. This configuration leads to an increase in the operational voltage window up to values of 1.8 V and consequently to a higher specific capacitance (200 F g⁻¹) and energy density (~25 Wh kg⁻¹). Four different mass ratios were employed (1, 1.5, 2 and 3), and the electrochemical response of the cells was evaluated by means of cyclic voltammetry, galvanostatic charge–discharge and impedance spectroscopy. The results demonstrate that the optimal carbon mass ratio in the electrodes is about 2.0 because in these conditions the devices are able to operate with a maximum cell voltage of 1.8 V and with a high electrical efficiency.

Keywords Carbon xerogel electrodes · Asymmetric configuration · Electrode loading · High voltage · Aqueous electrolyte

1 Introduction

Supercapacitors (SCs) are electrochemical energy storage systems that are characterized by a high power rate and long cycle lifetime with a high coulombic efficiency, i.e. a high reversibility and a low environmental impact [1–4]. With these properties, SCs can be used as energy storage devices in a large number of applications, especially where a high power is needed for a short time, as in the case of hybrid electric vehicles or emergency systems [1–4]. The main drawback of SCs is their restricted energy density, which is much smaller than that supplied by other energy storage systems such as batteries or fuel cells (e.g. 4–8 Wh kg⁻¹ for a commercial symmetric supercapacitor, from 10 to 50 Wh kg⁻¹ for an asymmetric SC based on a redox electrode and >100 Wh kg⁻¹ for Li-ion batteries [3]). Hence, a lot of the current research is directed towards developing more efficient SCs in terms of energy density.

From the equation used to calculate the energy density (E) of a supercapacitor:

$$E = \frac{1}{2} CU^2$$

where C is the capacitance in Farads and U the operating voltage, it can be seen that an efficient way to increase the E of SCs would be to develop highly and suitably porous electrode materials to enhance the capacitance and/or to extend the voltage stability window. The latter can be defined as the voltage range within which neither the electrode material nor the electrolyte undergo decomposition.

The maximum voltage of aqueous-based SCs is typically limited to ~1.0 V, due to the decomposition of water at 1.23 V, whereas SCs can be charged to a potential difference of 2.5 V or >3.5 V, when organic

E. G. Calvo (✉) · A. Arenillas · J. A. Menéndez
Instituto Nacional del Carbón CSIC, Apartado 73,
33080 Oviedo, Spain
e-mail: esthergc@incar.csic.es

E. G. Calvo · F. Lufrano (✉) · A. Brigandì · P. Staiti
Istituto di Tecnologie Avanzate per L'Energia "Nicola
Giordano", CNR-ITAE, Via Salita S. Lucia 5, 98126 Messina,
Italy
e-mail: lufrano@itae.cnr.it

solutions and ionic liquids are used as electrolytes [5–7]. From the point of view of the voltage stability window of the electrolyte, it is evident that aqueous media are less favourable for this application. Nevertheless, this medium offers many advantages over the other two types of electrolytes including its higher conductivity, low cost, easy preparation and handling and low environmental impact [5–7]. In recent years, different strategies have been adopted to extend the working voltage of SCs without having to replace aqueous solutions by other more expensive, complex and environmental unfriendly electrolytes. Some of these strategies have been aimed at the development of SCs, based on aqueous solutions, which are composed of two electrode materials that are able to operate within different potential ranges, thereby enhancing the stability window of the SCs. For example, some authors have developed asymmetric aqueous SCs that exhibit a voltage stability window close to 2.0 V by employing a carbonaceous material as negative electrode and an active material with pseudo-capacitive properties as positive electrode (e.g. carbon xerogel (–)/MnO₂ (+) [8]; activated carbon (–)/MnO₂ (+) [9]; activated carbon (–)/LiMn₂O₄ (+) [10]; activated carbon (–)/activated carbon fibres-PANI (+) [11]; MnO₂-AC (–)/Li₄Mn₅O₁₂ (+) [12], etc.). However, all of these proposals involve using two different active materials and, therefore, they lead to more expensive and less ecological SCs than those composed solely of carbon materials. This has led several researchers to consider the possibility of developing asymmetric SCs that employ the same nanoporous carbon in both electrodes but in unequal loads [13–16].

In 2012, some of the authors of the present paper published a study based on the preparation of an asymmetric supercapacitor that employed a highly porous carbon xerogel as active material with a mass ratio between the positive and negative electrode (m_+/m_-) close to 2 [16]. In the present work, we have gone a step further and have modified the m_+/m_- ratio with the aim of determining the optimal mass ratio that would result in a supercapacitor with a larger voltage window and a good electrochemical performance over a sizable number of charge–discharge cycles. For this purpose, four SCs with different mass ratios between both electrodes ($m_+/m_- = 1, 1.5, 2$ and 3) were assembled, using a micro-mesoporous carbon xerogel as active material in both electrodes and a sodium sulfate solution (1.0 mol L^{-1}) as electrolyte. The performance of the cells was evaluated by means of different electrochemical techniques (cyclic voltammetry (CV), galvanostatic charge/discharge (G-CD) and impedance spectroscopy).

2 Experimental

2.1 Electrode material

The active material selected for this study was a commercial carbon xerogel provided by Xerolutions (*XER-HSA-09*) (Oviedo, Spain). This carbon xerogel was obtained by means of polymerization reactions between resorcinol and formaldehyde monomers (the pH of the resorcinol/formaldehyde solution was 6.5), using microwave heating to favour the reactions [17, 18]. Once the microwave-induced synthesis had concluded, the material was subjected to an activation process using CO₂ as activating agent at $1,000^\circ\text{C}$ with a heating rate of $50^\circ\text{C min}^{-1}$, and this maximum temperature was kept for 2 h, in order to ensure the development of microporosity in the sample [19]. The porosity of the carbon xerogel was characterized from the N₂ adsorption–desorption isotherm at -196°C (*Micromeritics Tristar 3020*). Before the characterization, the sample was outgassed at 120°C overnight under vacuum. The specific surface area (S_{BET}) and micropore volume (V_{micro}) were calculated from the N₂ adsorption isotherm by means of the Brunauer–Emmett–Teller and Dubinin–Raduskevich equations, respectively. The total pore volume (V_{p}) was calculated from the N₂ adsorbed at saturation point ($p/p^\circ = 0.99$), and the mesopore volume (V_{meso}) was determined by subtraction ($V_{\text{p}} - V_{\text{micro}}$).

To investigate the chemical properties of the active material, it was subjected to elemental analysis tests. The amounts of C, N and H were calculated using a LECO-CHNS-932 microanalyzer, and the oxygen content was determined on a LECO-TF-900. The point of zero charge (PZC) was determined in order to facilitate the identification of the surface chemistry of the *XER-HSA-09* carbon xerogel.

2.2 The electrochemical response of asymmetric SCs

A series of square-shaped electrodes, with a surface of 4 cm^2 and a thickness of between 100 and $250 \mu\text{m}$, were prepared by mixing a slurry of carbon xerogel, graphite fibres, polyvinylidene fluoride in an organic solvent (*N,N*-dimethylacetamide). The mass ratio of the solid materials was fixed at 80:10:10. Once the composite electrodes were obtained, a drying step followed by a heat treatment at 160°C was carried out in order to improve the mechanical strength of the final electrodes. Four different ratios of carbon xerogel load between the positive and negative electrode were evaluated ($m_+/m_- = 1, 1.5, 2$ and 3), which means that the electrode density varied between a minimum value of 2.8 mg cm^{-2} and a maximum value of

8.4 mg cm⁻² (further information about the electrode density of the electrochemical cells is presented in Table 2).

All the electrochemical measurements were performed at room temperature using a two-electrode cell configuration (cells built with carbon xerogel-based electrodes separated by a porous paper approximately 60 µm thick and graphite plate current collectors). The electrolyte used in this work was a 1.0 mol L⁻¹ solution of Na₂SO₄. CV, and G-CD measurements were performed using a potentiostat/galvanostat *Autolab PGSTAT 30* (Eco Chemie, BV, The Netherlands). The operating conditions included a sweep rate of 100 mV s⁻¹ and a current density of 1.0 A g⁻¹ for the CV and G-CD measurements, respectively, within increasing voltage windows (from 0–1.0 to 0–2.0 V, with increments of 200 mV). The value of specific capacitance per one electrode (C_p) was obtained by G-CD measurements and calculated by the following equation:

$$C_p = C \frac{(m_a + m_c)}{m_a \cdot m_c}$$

where C is the capacitance (Farads) of the capacitor; m_a is the mass of active material in the anode, and m_c is the weight of active material in the cathode. C_p is obtained as a weighted average of the mass of active material in both electrodes, which is a more precise method to calculate the capacitance of one electrode when the masses and capacitances of two electrodes are different [8, 20].

In the case of the optimum m_+/m_- , a durability test was also conducted by applying a substantial number of galvanostatic charge–discharge cycles with a voltage range from 0 to 1.8 V and a current density of 5 A g⁻¹.

Impedance spectroscopy measurements were also performed on the two-electrode capacitors using the potentiostat *PGSTAT 30* equipped with a *FRA2* module. The measurements were carried out in open circuit voltage (OCV) conditions using an AC potential amplitude of 10 mV and a frequency range of 1 mHz–100 kHz.

3 Results and discussion

The data relating to the textural and chemical properties of the carbon xerogel used as electrode material are presented in Table 1. The *XER-HSA-09* sample is a micro-mesoporous material that has a very high BET surface area of almost 2,900 m² g⁻¹. Moreover, as can be seen from the table, the sample has a significant mesopore volume (i.e. $V_{\text{meso}} = 1.28 \text{ cm}^3 \text{ g}^{-1}$) and the mesopore size distribution (not included in this paper) comprises mesopore diameters ranging from 2 to 16 nm, pores that can favour the diffusion of the ions from the bulk of the electrolyte to the microporosity of the

electrode material, especially under fast polarization conditions [3, 5, 21–23]. In short, this carbon xerogel has textural properties that are highly suitable for the application proposed in this work.

Table 1 also summarizes the results obtained from the chemical characterization of the *XER-HSA-09* xerogel. As expected, the carbon xerogel is mainly composed of C (>97 wt%), although a very small amount of oxygen was detected (i.e. O = 2.1 wt%). According to these elemental analysis results, the carbon xerogel does not contain a large amount of oxygen surface groups, but the limited oxygen groups presented on the surface of the electrode material have a slightly basic nature, as the value of its PZC indicates (i.e. PZC = 8.3).

The first electrochemical studies conducted on the carbon xerogel-based SCs of different configurations were CV tests (sweep rate of 100 mV s⁻¹ and varying cell voltages). The voltammograms obtained from these measurements are shown in Fig. 1. As the shape of the curves of Fig. 1a evidences, the symmetric supercapacitor (i.e. when $m_+/m_- = 1$) experiences problems of charge propagation at a high scan rate of 100 mV s⁻¹, which are more pronounced than in the case of the asymmetric systems (i.e. when $m_+/m_- > 1$). Above 1.5 V, there is likely a slight decomposition of the electrolyte that becomes clearly apparent at 2.0 V.

This situation differs with the asymmetric configurations. When $m_+/m_- > 1$, the voltammograms show quasi-rectangular shaped profiles typical of cells with an almost pure capacitive behaviour, even when wide potential windows are used. When the mass ratio is set to 1.5 and 2.0, it is possible to use operation voltage ranges up to 1.8 V without any detectable electrolyte decomposition or other irreversible electrode reactions. However, when $m_+/m_- = 3$, significant humps appear during the anodic and cathodic scans, indicating that redox reaction are occurring. The humps in the voltammograms are particularly pronounced during the positive polarization above 1.5 V, when probably the water starts to decompose, and the hydrogen generated is adsorbed by the electrode material; this adsorbed hydrogen is then desorbed during the discharging step [6, 24]. Consequently, the hydrogen produces a pseudocapacitance during the sorption/desorption process on the carbon surface, which acts as additional capacitance to the electric double layer capacitance. However, because the non-Faradaic (EDLC) and Faradaic (redox) processes have different time constants, the latter can only be observed under specific experimental conditions. Thus, when $m_+/m_- = 3$, the negative electrode is forced to work under a high overpotential of ~1.3 V whereas the positive electrode functions at ~0.5 V, so that the peaks showed in the voltammograms of the full capacitor are to be attributed mainly to processes that occur on the negative electrode.

Table 1 Textural and chemical properties of the carbon xerogel used as electrode material

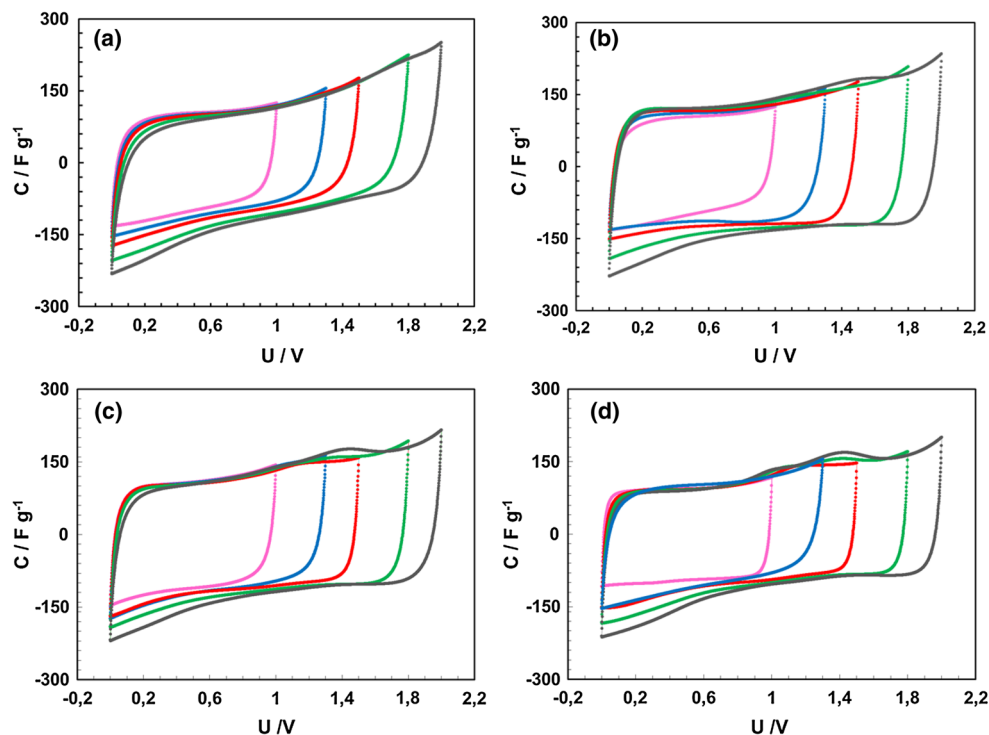
| N ₂ adsorption–desorption (77 K) | | | Elemental analysis (wt% db ^c) | | | | PZC |
|--|---|--|---|-----|-----|-----|-----|
| S_{BET} (m ² g ⁻¹) | V_{micro}^a (cm ³ g ⁻¹) | V_{meso}^b (cm ³ g ⁻¹) | C | H | O | N | 8.3 |
| 2,876 | 0.97 | 1.28 | 97.5 | 0.3 | 2.1 | 0.1 | |

^a Obtained by applying the Dubinin–Raduskevich equation to the N₂ adsorption isotherm

^b $V_{\text{meso}} = V_{\text{p}} - V_{\text{micro}}$, where V_{p} is the adsorbed volume at saturation point ($p/p^\circ = 0.99$)

^c Dry basis

Fig. 1 Cyclic voltammograms obtained at 100 mV s⁻¹ in two-electrode cells. Mass ratio = 1 (a), 1.5 (b), 2.0 (c) and 3.0 (d)



These preliminary results obtained by CV suggest that it is possible, in certain conditions, to operate at a voltage higher than 1.23 V, which is considered the upper limit for aqueous electrolytes due to water decomposition.

The characteristics of the electrodes and the electrochemical results of the carbon xerogel-based SCs are reported in Table 2. The characteristics of the cells vary according to the different mass ratios between the positive and negative electrode, since these have a noticeable influence on their electrochemical performance. Each supercapacitor (symmetric and asymmetric) was loaded with active material (micro-mesoporous carbon xerogel) ranging from 39 to 47 mg. Depending on the load of active material, the thickness and density of the carbon electrodes were slightly modified resulting in capacitances (Farad), and volumetric capacitances (F cm⁻³) that changes according to the different mass ratios used. A higher capacitance as well as higher volumetric capacitance, energy and power density were reported when $m_+/m_- = 1$,

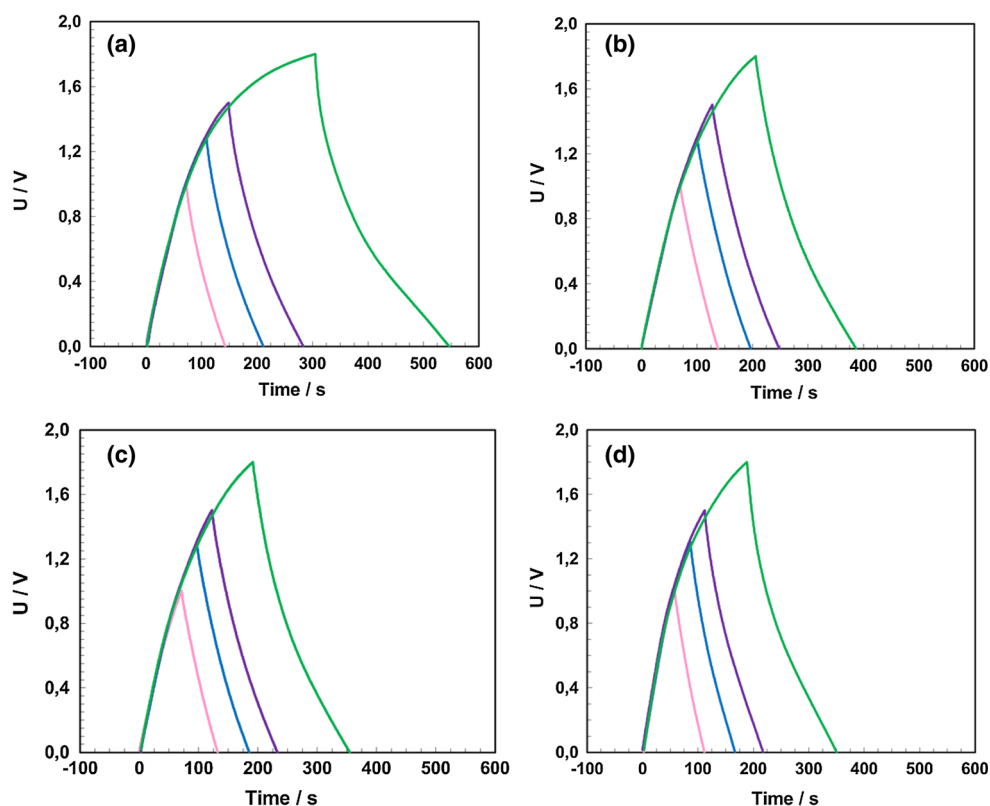
even though this SC is associated with a worse coulombic efficiency (coulombic efficiency is defined as the percentage of charge stored during the charge cycle and that recovered during the discharge cycle) than the asymmetric SCs.

Therefore, the symmetric SC, even despite having the highest values of capacitance and energy and power density, did not exhibit the best overall electrochemical characteristics. A more effective comparison was obtained by considering the properties just mentioned together with the results obtained from the galvanostatic charge–discharge.

In order to further assess the electrochemical performance of the SCs, galvanostatic charge–discharge experiments at a high current load of 1 A g⁻¹ and in increasing voltage windows were performed (see Fig. 2). The chronopotentiograms reveal that the asymmetric SCs showed a better electrochemical behaviour than the symmetric systems when high operating voltages were used. Up to 1.5 V, the three asymmetric cells displayed almost symmetric

Table 2 Characteristics of investigated electrodes and electrochemical performance for the four carbon xerogel-based asymmetric supercapacitors

| Mass ratio ^a (m_+/m_-) | Carbon (mg cm^{-2}) | Electrode thickness (μm) | R_{imp}^b ($\Omega \text{ cm}^2$) | Farad by GCD ^c | $F \text{ cm}^{-3}$ | E_{max}^d (Wh kg^{-1}) | P_{max}^d (kW kg^{-1}) |
|--|-----------------------------------|--|---|------------------------------|---------------------|---|---|
| 1.0 | 5.14 | 210 | 0.34 | 2.64 | 15.0 | 30.0 | 240.6 |
| | 4.76 | 180 | | | | | |
| 1.5 | 7.12 | 230 | 0.29 | 2.40 | 13.0 | 23.7 | 237.1 |
| | 4.74 | 180 | | | | | |
| 2.0 | 6.46 | 220 | 0.37 | 1.79 | 11.5 | 22.8 | 224.6 |
| | 3.34 | 120 | | | | | |
| 3.0 | 8.40 | 240 | 0.31 | 2.02 | 12.6 | 27.1 | 196.5 |
| | 2.80 | 110 | | | | | |

^a Mass ratio between the positive and negative electrode^b Cell resistance by impedance analysis; cell size = 4 cm^2 ^c Current density = 1 A g^{-1} ^d Parameters obtained from the galvanostatic test at 1 A g^{-1} and $U = 1.8 \text{ V}$ **Fig. 2** Galvanostatic charge–discharge curves measured with a current density of 1 A g^{-1} . $R = 1.0$ (a), $R = 1.5$ (b), $R = 2.0$ (c) and $R = 3.0$ (d)

charge and discharge curves, suggesting that the electrodes possess a high capacitive performance and a good electrochemical cycle reversibility. However, when the voltage range was raised to 1.8 V , a distortion in the linearity due to pseudo-capacitive effects was observed.

The progression of specific capacitance (expressed as Farads per gram of active material, considering the average mass between both electrodes) as a function of the

operating voltage is shown in Fig. 3. In addition, Fig. 4 shows the coulombic efficiency values obtained from the same electrochemical measurements.

The results in Fig. 3 reveal that there are virtually no differences between the specific capacitance values obtained in the four cases tested when the cell voltage is 1.0 V (C values of around 140 F g^{-1}), due to the fact that the systems are operating in the region of electrochemical

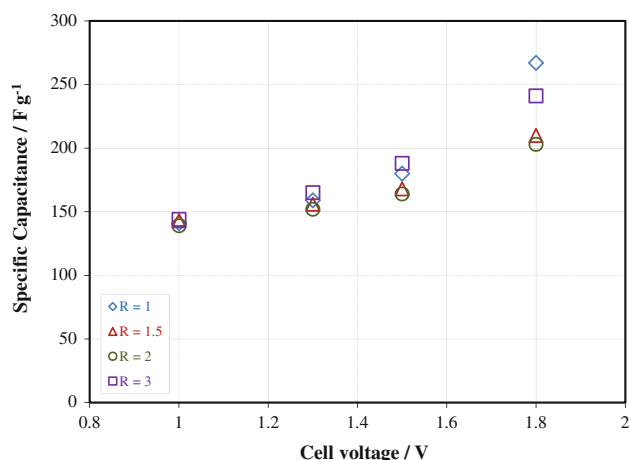


Fig. 3 Specific capacitance versus voltage for the asymmetric systems obtained from GCD measurements in the two-electrode cell. The cells were charged and discharged at 1 A g^{-1}

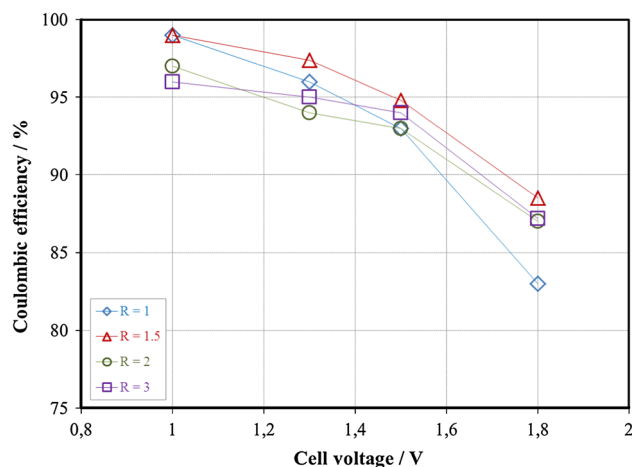


Fig. 4 Coulombic efficiency as a function of operating voltage for the asymmetric systems evaluated

stability of water. As there is no extra pseudo-capacitance, the four SCs are able to store the same amount of charge. However, the results obtained differ at higher operating voltages, and these discrepancies between the SCs are accentuated as the cell voltage increases. It is important to note that in the case of the two larger voltage windows (i.e. $\Delta V = 1.5$ and 1.8 V), the symmetric supercapacitor ($m_+/m_- = 1$) and the corresponding asymmetric cell with $m_+/m_- = 3$ are capable of storing a greater amount of energy (i.e. 270 and 240 F g^{-1} when $m_+/m_- = 1$ and 3 , respectively, compared to a capacitance of around 200 F g^{-1} in the case of the other two mass ratios tested). However, this higher energy storage capacitance can be attributed to a pseudocapacitance arising from redox reactions on the carbon surface, which is consistent with the results obtained from the CV and charge–discharge curves

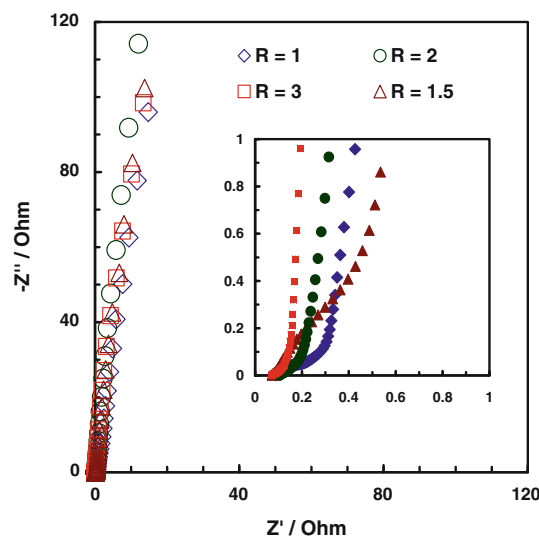


Fig. 5 Nyquist plots for two-electrode cells with the four different electrode mass ratio used. The inset shows the high frequency region of impedance

discussed in the previous paragraphs. Therefore, despite achieving a value of specific capacitance as high as that obtained when m_+/m_- is set to 1 and 3 , the use of wide voltage ranges with those SCs would not be possible because there is an important contribution of pseudocapacitive effects and, therefore, these electrochemical systems are not stable.

The coulombic efficiency data collected in Fig. 4 reflect the worse electrochemical performance of the symmetric supercapacitor, SC, when a high cell voltage was used (i.e. when $\Delta V = 1.8 \text{ V}$, the efficiency of the SC was below 85%). As demonstrated with Fig. 3, this supercapacitor provides a higher gravimetric capacitance than the corresponding asymmetric cells, but this is due to redox reactions produced by water oxidation/reduction, which results in a poorer efficiency. These results demonstrate that the use of asymmetric systems with unequal loads of carbon in the electrodes is a good strategy, since it allows an increase in the operating voltage, using a cheap and environmental friendly aqueous electrolyte while ensuring, at the same time, a sufficiently high coulombic efficiency.

Electrochemical impedance spectroscopy measurements were performed in the frequency range of 100 kHz to 1 mHz on the different capacitors operating with an OCV and unequal carbon xerogel load in the electrodes. The Nyquist plots of the SCs in Fig. 5 present typical capacitive shapes of data points distributed near a vertical line at medium and low frequency intervals. The slight inflexion from the vertical line is assigned to the resistive behaviour of real SCs. The resistive effect can be imagined as the difficulty of penetration of the electric signal in smaller pores and filling of the ions (electrolyte) into the narrow

Table 3 Comparison of electrochemical performance of our carbon-based asymmetric supercapacitor with literature data

| Reference | Active material | S_{BET} ($\text{m}^2 \text{g}^{-1}$) | R (m_+/m_-) | Voltage (V) | Electrolyte | C (F g^{-1}) |
|-----------|--------------------|---|-------------------|-------------|------------------------------|---------------------------|
| This work | Carbon xerogel | 2,876 | 2.0 | 1.8 | Na_2SO_4 | 200 |
| [11] | AC (–) | 2,905 (–) | – | 1.6 | H_2SO_4 | 85 |
| | ACF-PANI (+) | 925 (+) | | | | |
| [13] | Cabot Monarch | 1,300 | 4:3 | 1.9 | K_2SO_4 | 80 |
| [14] | Norit S50 oxidized | 1,382 | 2.0 | 1.5 | H_2SO_4 | 136 |
| | | | | 1.0 | KOH | 133 |
| [15] | Carbon xerogel | 600 ^a | >1 | 3.4 | $\text{PYR}_{14}\text{TFSI}$ | 26 ^b |
| | | | | 3.7 | EMITFSI | 21 ^b |
| [16] | Carbon xerogel | 3,100 | 2.1 | 1.8 | Na_2SO_4 | 156 |

AC activated carbon, ACF-PANI activated carbon fibres/polyaniline

^a Specific surface area related to pores wider than 1.5 nm^b Specific capacitance for the global supercapacitor

carbon pores with the increasing time. An ideal electric double layer should have a quasi-instantaneous charge redistribution (electric and ionic) in the electrodes, but the porous nature of the electrodes, the ionic redistribution of cations (Na^+) in the negative electrode and the anions (SO_4^{2-}) in the positive electrode will occur at different time constants. To quantify the deviation from the ideal behaviour of these capacitors, it is necessary to consider that the resistances range from 0.070–0.090 (Ω) at high frequency ~ 100 kHz) to 10–20 Ω (at low frequency 1 mHz) as a function of the characteristics of the SCs. The cells loaded with $m_+/m_- = 2$ and 3 show higher resistances than those loaded with $m_+/m_- = 1$ and 1.5. These differences are mainly assigned to the small thickness of the electrodes. The electric series resistances (ESR) (high frequency region) of the cells oscillate between 0.29 ($m_+/m_- = 1.5$) and 0.37 Ωcm^2 when $m_+/m_- = 2$, and they are attributed to the ionic resistance of the electrolyte (which is the largest), the intrinsic resistance of the carbon electrodes and the contact resistances between the interfaces of the active material electrode/current collector.

In a first approximation, we have estimated 70–90 % resistance as being due to the electrolyte/separator, 12–20 % to the electrodes and 6–12 % to the interface/current collectors. These approximate values were based on the results of a previous study [25], in which the different components of ESR were separated by studying various SCs. It was shown that the ESR increased with the increase in electrode thickness according to the different carbon loads in the electrodes. The variation of the ESR of electrodes of greater thickness allowed the ionic resistance of the electrolyte to be separated from that of the carbon composite electrodes.

Deviation from the ideal capacitor (e.g. non-vertical line in the Nyquist plots) and the increase in resistance when the frequency descends from 100 MHz to 1 mHz does not

detract from the quality of the investigated SCs. As can be seen in the inset of Fig. 5, the ESR (high frequency region) of the cells varied from 0.29 ($m_+/m_- = 1.5$) to 0.37 Ωcm^2 ($m_+/m_- = 2$). The very low values of the resistances and the high capacitances reported in this study compared favourably with previous results reported in other papers [4, 26, 27]. In fact, Stoller et al. [26] reported for graphene-based symmetric SCs values of ESR resistances of 0.30, 1.28 and 1.3 Ωcm^2 using 1 mol L^{-1} NaOH, TEABF₄/PC and TEABF₄/AN electrolytes, respectively. Their electrode thicknesses were ~ 75 μm with a cell size of 2 cm^2 . The same group reported for SCs based on a chemical activated graphene (a-MEGO, BET SSA $\sim 3,100 \text{ m}^2 \text{g}^{-1}$), ESR values of 3 Ωcm^2 with 1 mol L^{-1} TEABF₄/AN electrolyte [4]. Their electrode thicknesses were of the order of 40–50 μm , and the cell size was 1 cm^2 . The specific capacitance calculated from the discharge curves was 154 F g^{-1} for a current of 0.8 A g^{-1} [4]. Similarly, Fic et al. [27] reported for symmetric aqueous SCs ($\sim 0.785 \text{ cm}^2$ cell size) in 1 mol L^{-1} Li_2SO_4 and Na_2SO_4 , specific resistance values of 0.45 and 0.55 Ωcm^2 , respectively. They reported gravimetric capacitance values of 140 F g^{-1} in Li_2SO_4 and 110 F g^{-1} in Na_2SO_4 with activated carbon electrodes. In short, our results of $\sim 200 \text{ F g}^{-1}$ for $m_+/m_- = 2$ and $\sim 235 \text{ F g}^{-1}$ for $m_+/m_- = 3$ in 1 mol L^{-1} Na_2SO_4 reported here compare favourably with the current state of the art, especially considering the low electric series resistance (ESR) of $\sim 0.3 \Omega \text{cm}^2$ achieved with the asymmetric aqueous supercapacitors used in this study.

Table 3 provides a comparison between the electrochemical behaviour of one of the asymmetric SCs prepared in this work ($m_+/m_- = 2$) and other asymmetric devices composed of various carbonaceous materials reported in the literature. The specific capacitance values reported in this work are greater than the literature data, and this can be

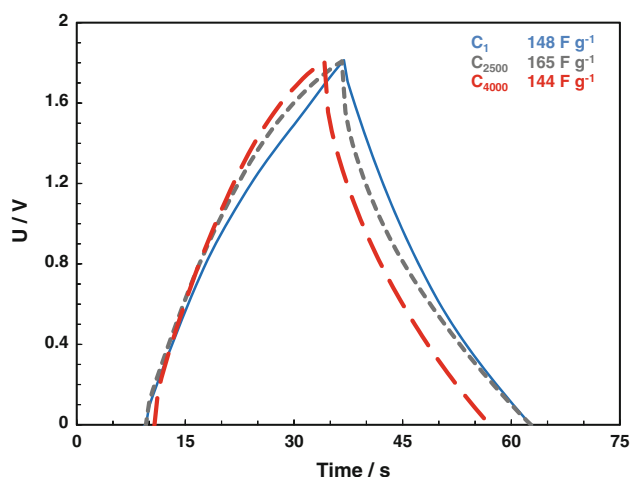


Fig. 6 Cycleability studies for the carbon xerogel-based supercapacitor when $m_+/m_- = 2$ (voltage range: 1.8 V; current density: 5 A g⁻¹)

attributed to the nature of the active material used for the electrodes. Carbon xerogels are materials characterized by their porous properties that are highly suitable for energy storage application due to their high surface area (S_{BET} larger than a lot of commercial activated carbons) and the presence of mesopores that has a positive effect on charge storage processes since the rapid diffusion of electrolyte ions is promoted by this kind of porosity. If the specific capacitance value of 200 F g⁻¹ is compared with that of 156 F g⁻¹ obtained from Ref. [16], it can be observed that the energy storage capacitance obtained with our supercapacitor is higher although these authors also used a highly porous carbon xerogel. This may be related to the particular porous structure of the resorcinol–formaldehyde carbon xerogel used in the present work, while the active material used by the other authors was a highly microporous carbon xerogel with a low mesopore volume, which might explain its lower value of specific capacitance. According to this table, it is clear that it is possible to extend the voltage stability window using unequal mass electrodes, without the need to replace environmental friendly aqueous solutions by non-aqueous organic electrolytes or ionic liquids. Also of importance are the type of active material and the mass ratio between the positive and negative electrode used because they influence the storage capacitance and voltage range and, thereby, energy and power density values.

The cycling performance of the *XER-HSA-09* carbon xerogel-based supercapacitor ($m_+/m_- = 2$) collected in Fig. 6 reveals that the electrode retains ~100 % of specific capacitance after 4,000 charge–discharge cycles ($U = 1.8$ V and a current density as high as 5 A g⁻¹). Even after 2,500 cycles, the specific capacitance value has been slightly increased (168 F g⁻¹). These results

demonstrate that the carbon xerogel-based asymmetric supercapacitor is suitable for high rate and highly stable devices.

4 Conclusions

Asymmetric SCs prepared with carbon xerogel-based electrodes of different carbon loads were assembled and investigated in this work. A working voltage as high as 1.8 V, with a good coulombic efficiency and a high energy storage capacitance, was achieved using unequal mass carbon electrodes and a Na₂SO₄ solution (1 mol L⁻¹) as electrolyte. Of the four positive/negative mass ratios evaluated ($m_+/m_- = 1, 1.5, 2$ and 3), the results reveal that the optimum mass ratio is around 2, since this cell provides a high coulombic efficiency, and it operates effectively at a cell voltage of 1.8 V over a large number of charge–discharge cycles, without producing any appreciable electrolyte decomposition or irreversible processes in the electrodes. The specific capacitance reported for this asymmetric cell was above 200 F g⁻¹, a value that is higher than those reported in the literature with similar asymmetric devices. SCs assembled with a $m_+/m_- = 1$ and 3 display the highest values of specific capacitance. However, the results obtained from CV, galvanostatic charge–discharge tests and impedance spectroscopy evidence the instability of these electrochemical cells when they are operating at 1.8 V.

On the basis of these results, it is clear that the manufacture of asymmetric SCs consisting of electrodes of different mass based on a highly porous carbon xerogel is a good strategy for solving the main problem associated with SCs, i.e. their low E compared to other energy storage devices, because higher voltage stability window in aqueous electrolytes could be used.

Acknowledgments The authors of INCAR-CSIC would like to acknowledge the financial support provided by the Ministerio de Economía y Competitividad (Ref. MAT-2011-23733 and IPT-2012-0689-420000). The authors of CNR-ITAE acknowledge the financial support provided by Ministero dello Sviluppo Economico within the framework of ‘Accordo ti programma CNR-MSE’, project ‘Sistema elettrochimici per l’accumulo dell’energia’. The COST Organization (COST Action MP1004: Hybrid Energy Storage Devices and Systems for Mobile and Stationary Applications) is also gratefully acknowledged. E.G. Calvo also thanks Ficyt (Spain) for a predoctoral research grant.

References

1. Kötter R, Carlen M (2000) Principles and applications of electrochemical capacitors. *Electrochim Acta* 45:2483–2498
2. Pandolfo AG, Hollenkamp AF (2006) Carbon properties and their role in supercapacitors. *J Power Sources* 157:11–27

3. Xin L, Bingqing W (2013) Supercapacitors based on nanostructured carbon. *Nano Energy* 2:159–173
4. Zhu Y, Murali S, Stoller MD, Ganesh KJ, Cai W, Ferreira PJ, Pirkle R, Wallace M, Cychosz KA, Thommes DS, Stach EA, Ruoff RF (2011) Carbon-based supercapacitors produced by activation of graphene. *Science* 332:1537–1541
5. Demarconnay L, Calvo EG, Timperman L, Anouti M, Lemordant D, Raymundo-Piñero E, Arenillas A, Menéndez JA, Béguin F (2013) Optimizing the performance of supercapacitors based on carbon electrodes and protic ionic liquids as electrolytes. *Electrochim Acta* 108:361–368
6. Frackowiak E, Abbas Q, Béguin F (2013) Carbon/carbon supercapacitors. *J Energy Chem* 22:226–240
7. Lewandowski A, Olejniczak A, Galinski M, Stepniak I (2010) Performance of carbon–carbon supercapacitors based on organic, aqueous and ionic liquid electrolytes. *J Power Sources* 195:5814–5819
8. Lufrano F, Staiti P, Calvo EG, Juárez-Pérez EJ, Menéndez JA, Arenillas A (2011) Carbon xerogel and manganese oxide capacitive materials for advanced supercapacitors. *Int J Electrochem Sci* 6:596–612
9. Yuan A, Zhang Q (2006) A novel hybrid manganese dioxide/activated carbon supercapacitor using lithium hydroxide electrolyte. *Electrochem Commun* 8:1173–1178
10. Wang YG, Xia YY (2005) A new concept hybrid electrochemical supercapacitor: carbon/LiMn₂O₄ aqueous system. *Electrochem Commun* 7:1138–1142
11. Salinas-Torres D, Sieben JM, Lozano-Castelló D, Cazorla-Amorós D, Morallón E (2013) Asymmetric hybrid capacitors based on activated carbon and activated carbon fibre-PANI electrodes. *Electrochim Acta* 89:326–333
12. Chu HY, Lai QY, Hao YJ, Zhao Y, Xu XY (2009) Study of electrochemical properties and the charge/discharge mechanism for Li₄Mn₅O₁₂/MnO₂-AC hybrid supercapacitor. *J Appl Electrochem* 39:2007–2013
13. Chae JH, Chen GZ (2012) 1.9 V aqueous carbon–carbon supercapacitors with unequal electrode capacitances. *Electrochim Acta* 86:248–254
14. Khomenko V, Raymundo-Piñero E, Béguin F (2010) A new type of high energy asymmetric capacitor with nanoporous carbon electrodes in aqueous electrolyte. *J Power Sources* 195:4234–4241
15. Lazzari M, Soavi F, Mastragostino M (2008) High voltage, asymmetric EDLCs based on xerogel carbon and hydrophobic IL electrolytes. *J Power Sources* 178:490–496
16. Staiti P, Arenillas A, Lufrano F, Menéndez JA (2012) High energy ultracapacitor based on carbon xerogel electrodes and sodium sulfate electrolyte. *J Power Sources* 214:137–141
17. Arenillas A, Menéndez JA, Zubizarreta L, Calvo EG (2009) Procedimiento de obtención de xerogeles orgánicos de porosidad controlada. Patent ES 2 354 782
18. Calvo EG, Juárez-Pérez EJ, Menéndez JA, Arenillas A (2011) Fast microwave-assisted synthesis of tailored mesoporous carbon xerogels. *J Colloid Interface Sci* 357:541–547
19. Calvo EG, Lufrano F, Staiti P, Brigandì Arenillas A, Menéndez JA (2013) Optimizing the electrochemical performance of aqueous symmetric supercapacitors based on an activated carbon xerogel. *J Power Sources* 241:776–782
20. Fang QL, Evans DA, Roberson SL, Zheng JP (2001) Ruthenium oxide film electrodes prepared at low temperatures for electrochemical capacitors. *J Electrochem Soc* 148:A833–A837
21. Frackowiak E (2007) Carbon materials for supercapacitor application. *Phys Chem Chem Phys* 9:1774–1785
22. Li X, Liu L, Meng Q, Cao B (2012) Synthesis and characterization of carbon aerogels doped with the anatase form of titanium oxide. *J Appl Electrochem* 42:249–254
23. Rasines G, Lavela P, Macías C, Haro M, Ania CO, Tirado JL (2012) Electrochemical response of carbon aerogel electrodes in saline water. *J Electroanal Chem* 671:92–98
24. Jurewicz K, Frackowiak E, Béguin F (2004) Towards the mechanism of electrochemical hydrogen storage in nanostructured carbon materials. *Appl Phys A* 78:981–987
25. Lufrano F, Staiti P, Minotuli (2004) Influence of Nafion content in electrodes on performance of carbon supercapacitors. *J Electrochem Soc* 151:A64–A68
26. Stoller MD, Park S, Zhu Y, An J, Ruoff RS (2008) Graphene-based ultracapacitors. *Nano Lett* 8:3498–3502
27. Fic K, Lota G, Meller M, Frackowiak E (2012) Novel insight into neutral medium as electrolyte for high-voltage supercapacitors. *Energy Environ Sci* 5:5842–5850